Dalton Transactions

Cite this: DOI: 10.1039/c2dt30618b

www.rsc.org/dalton

PAPER

Synthesis and characterisation of neutral mononuclear cuprous complexes based on dipyrrin derivatives and phosphine mixed-ligands†‡

Xiaohui Liu,[a,b] Hongmei Nan,*[c] Wei Sun,[a,d] Qikai Zhang,[d] Mingjian Zhan,[a] Luyi Zou,[a] Zhiyuan Xie,[a] Xiao Li,[a] Canzhong Lu[d] and Yanxiang Cheng*[a]

Received 19th March 2012, Accepted 29th May 2012
DOI: 10.1039/c2dt30618b

Heteroleptic neutral mononuclear cuprous complexes with dipyrrin derivatives and phosphine mixed-ligands including 1,3,7,9-tetramethyldipyrrin (**1**), 5-phenyl-1,3,7,9-tetramethyldipyrrin (**2**), 2,8-dibromo-1,3,7,9-tetramethyldipyrrin (**3**), 1,9-dichloro-5-phenyldipyrrin (**4**), 1,9-dibromo-5-phenyldipyrrin (**5**), 5-pentafluorophenyl-1,3,7,9-tetramethyldipyrrin (**6**) and 1,5,9-triphenyldipyrrin (**7**) have been synthesized and fully characterized. The central Cu(I) atoms of these complexes in general formulas of Cu(**1–6**)-$(PPh_3)_2$ (**1a–6a**) and Cu(**1–6**)(DPEphos) (**1b–6b**) [DPEphos = bis(2-diphenylphosphinophenyl)ether] all exhibit a pseudo-tetrahedral geometry, while complex Cu(**7**)(PPh_3) (**7a**) is tricoordinated in a pyramidal conformation due to the large steric hindrance of ligand **7**. The oxidation potentials assigned to oxidations of Cu(I)–Cu(II) are extraordinarily low in the range of 0.36–1.02 V *vs*. Ag/AgCl compared with traditional $[Cu(phen)(PP)]^+$ analogues. Their emission maxima range from 495 to 595 nm in dichloromethane at room temperature with quantum yields of 0.05–4.03% and lifetimes on the order of nanoseconds. Unlike the characteristic MLCT emission in cationic Cu(I) complexes, the emissions are assigned to the dipyrrin-centered intraligand charge transition (ILCT) based on the fact that the increased conjugation within the dipyrrinato anion leads to a weaker metal–ligand interaction, thus preventing the mixing of π orbitals of ligand and 3d orbitals of Cu(I) atom. This conclusion is also supported by electrochemical data and theoretical calculations.

Introduction

Cuprous complexes as more cost-effective emitters have received more attention since their similar phosphorescent characteristics to the noble metal complexes at room temperature were observed.[1] Relative to the Cu(I)-bisphenanthrolines of low quantum yield,[2] mixed-ligand Cu(I) complexes containing phosphines have shown improved luminescence properties and practical potential in the application of electroluminescent devices and sensors.[3] Although these cationic complexes are of benefit to light-emitting electrochemical cells (LECs) fabricated by solution processing,[3,4] their inherent defects from the counteranion would cause some problems in practical applications, such as unsuitability for sublimation and vapor deposition processing.[3] Therefore, an increasing number of neutral cuprous complexes have been developed using non-traditional 1,10-phenanthroline ligands, which achieved some better performances in their photophysical properties and applications.[5] Recently, Eisenberg's group reported a series of neutral Cu(I) complexes based on sp^3 N atom negative ligands, which exhibit characteristic phosphorescent emission from the mixed intraligand and metal-to-ligand charge transfer transition (ILCT and MLCT).[6] An interesting property of the neutral Cu(I) complexes as oxygen sensors have also been observed in our group with good reversibility through energy and electron transfer mechanisms.[7]

BODIPY (boron difluoride dipyrromethene) and it derivatives are widely used as molecular probes and label dyes in environmental chemistry and biochemistry due to their strong molar absorbance and sharp emission with a high quantum yield.[8] The corresponding ligand, dipyrrin as a mono-anionic chelate, is very suitable to prepare metal complexes, especially for low oxidation state metal ions, such as Cu(I). Furthermore, its aromatic structure from a large conjugated backbone is a favorable factor to obtain luminescent complexes. In fact, plenty of dipyrrinato metal complexes have been reported.[8b] Among them, some

[a]*State Key Laboratory of Polymer Physics and Chemistry, Changchun Institute of Applied Chemistry, Chinese Academy of Sciences, Changchun 130022, P.R. China. E-mail: yanxiang@ciac.jl.cn; Fax: +86-431-85262572; Tel: +86-431-85262106*
[b]*The Graduate School, Chinese Academy of Sciences, Beijing 100039, P.R. China*
[c]*The First Affiliated Hospital, Changchun University of Chinese Medicine, Changchun 130021, P.R. China*
[d]*State Key Laboratory of Structural Chemistry, Fujian Institute of Research on the Structure of Matter, Chinese Academy of Sciences, Fuzhou 350002, P.R. China*

† Dedicated to Professor Dr Max Herberhold on the occasion of his 75th birthday.

‡ Electronic supplementary information (ESI) available: Absorption and emission spectra Fig. S1–S15, and cyclic voltammogram Fig. S16–S22. CCDC reference numbers 871234–871241. For ESI and crystallographic data in CIF or other electronic format see DOI: 10.1039/c2dt30618b

exhibit fluorescent emission with lifetime of nanoseconds, such as Zn(II)[9] and group 13 Al(III),[10] Ga(III) and In(III) dipyrrinato complexes.[10,11] Recent examples of noble-metal Ru(II),[12] Ir(III)[13] and Pt(II)[14] complexes, in contrast, display the expected phosphorescence with lifetime of microseconds. These results offer a good chance to explore the properties of neutral dipyrrinato cuprous complexes. Herein, we report the synthesis and characterisation of heteroleptic neutral cuprous complexes based on the dipyrrinato anion and auxiliary phosphine ligands. The dipyrrins with different substituent patterns including halogen atoms were chosen for investigating the photophysical properties of their Cu(I) complexes as a function of the effects of electronic structure and steric hindrance.

Experimental

General

Starting materials were purchased from Sigma-Aldrich, Acros or Fluka and used without further purification. Solvents were freshly distilled over appropriate drying reagents under argon atmosphere. All experiments were carried out under a dry argon atmosphere using standard Schlenk techniques unless otherwise stated.

Characterization. ^{1}H and $^{13}C\{^{1}H\}$ NMR with TMS as internal reference, $^{19}F\{^{1}H\}$ NMR with fluorobenzene as external reference, and $^{31}P\{^{1}H\}$ NMR spectra with 85% H_3PO_4 as external reference were recorded on a Bruker Avance 300 or 600 MHz spectrometer at room temperature. Elemental analyses for C, H and N were performed with a BioRad elemental analysis system. Absorption spectra were recorded on a Perkin-Elmer Lambda35 UV/Vis Spectrometer. Photoluminescence spectra were recorded on a Perkin L350 Spectrofluorophotometer. The PL quantum yields were determined by the integrating sphere with 409 nm excitation of a HeCd laser. Luminescence lifetimes were measured with a Lecroy Wave Runner 6100 digital oscilloscope (1 GHz) using a tunable laser (pulse width = 4 ns, gate = 50 ns) for the excitation (Continuum Sunlite OPO). The samples for all the steady optical spectra were in sealed quartz cuvettes under nitrogen atmosphere. Cyclic voltammetry was performed using the Chi660b electrochemical analyzer with a three-electrode cell in dry dichloromethane solution under an argon atmosphere. A glassy carbon working electrode, a Pt auxiliary electrode and a Ag–AgCl reference electrode were employed. The supporting electrolyte was 0.1 M tetrabutylammonium perchlorate (Bu_4NClO_4). Ferrocene was used as a standard to calibrate the system. The scan rate was 50 mV s^{-1}. DFT calculations were performed using the GAUSSIAN 03W software package using a spin-restricted formalism at the B3LYP level.[15] The basis sets 6-311++G** were used for H, C, N, O, F, P and Cl atoms, and Lanl2DZ basis sets for Br and Cu atoms. The HOMO and LUMO energies were determined using XRD geometries to approximate the ground state.

Crystal structure determinations. Single-crystal X-ray measurements were carried out on a Bruker SMART APEX CCD diffractometer equipped with a graphite monochromator and Mo-Kα radiation (λ = 0.71073 Å). Absorption corrections were applied using the SADABS program.[16] The structures were solved by direct methods and refined on F^2 using full matrix least-squares methods (SHELXS97 and SHELXL97 programs).[17] For complexes **4a**, **5a** and **7a** the data sets was corrected using the program SQUEEZE. All non-hydrogen atoms were refined anistropically. The positions of the hydrogen atoms attached to carbon atoms were fixed at their ideal positions. Table 1 summarizes crystallographic data for the dipyrrinato cuprous complexes reported here.

3,5-Dimethylpyrrole-2-carbaldehyde. The compound was synthesized using a similar method to that reported in the literature.[18] Freshly distilled $POCl_3$ (10.25 ml; 0.11 mol) was added dropwise to anhydrous DMF (8.5 ml; 0.11 mol) at 0 °C. The resulting solution was stirred for 15 min after the ice-bath was removed. Dry 1,2-dichloroethane (20 ml) was then added, and the solution was cooled to 0–5 °C. 2,4-Dimethylpyrrole (9.51 g, 0.10 mol) dissolved in dry 1,2-dichloroethane (20 ml) was added. Following the addition, the yellow mixture was heated to reflux for 15 min before being cooled to room temperature. Aqueous sodium acetate (45 g in 100 ml water) was then added (slowly at first then as rapidly as possible). The mixture was again refluxed for 15 min with vigorous stirring. The layers were separated, and the aqueous layer was washed three times with dichloromethane. The combined organic layer was washed three times with saturated brine, dried over Na_2SO_4, and evaporated under vacuum to give an oily liquid. The crude product was purified *via* chromatography on Al_2O_3 with petroleum ether to yield light yellow crystals (10.2 g, 82%). ^{1}H NMR (600 MHz, $CDCl_3$) δ 10.27 (s, 1H), 9.44 (s, 1H), 5.83 (s, 1H), 2.30 (s, 3H), 2.29 (s, 3H); ^{13}C NMR (151 MHz, $CDCl_3$) δ 175.89, 138.74, 134.86, 128.75, 112.01, 13.13, 10.58.

(3,5-Dimethylpyrrol-2-yl)(phenyl)methanone. 2,4-Dimethylpyrrole (8.10 g; 0.085 mol) in dry ether (150 ml) was added dropwise to a solution of ethylmagnesium bromide in ether (0.094 mmol, 1.1 eq.) so as to cause slight reflux. The solution was refluxed for an additional 30 min. A solution of benzoyl chloride (9.87 ml, 0.085 mol) in dry ether (30 ml) was dropped to the reaction solution. The orange suspension was heated to reflux for 2 h, and poured into saturated aqueous ammonium chloride. The precipitate was dissolved in CH_2Cl_2 and washed with water (150 ml × 3), dried over Na_2SO_4, and evaporated to give a red oil. The oil was purified *via* chromatography on a silica gel flash column with 4 : 1 petroleum ether–EtOAc as eluent to yield an orange solid. Recrystallization from petroleum ether gave the product as white crystals (13.30 g, 79%). ^{1}H NMR (600 MHz, $CDCl_3$) δ 9.73 (s, 1H), 7.64–7.60 (m, 2H), 7.51–7.45 (m, 1H), 7.42 (t, J = 7.4 Hz, 2H), 5.84 (d, J = 2.6 Hz, 1H), 2.28 (s, 3H), 1.90 (s, 3H); ^{13}C NMR (151 MHz, $CDCl_3$) δ 185.79, 140.28, 136.10, 130.82, 128.23, 128.20, 127.84, 112.97, 14.03, 13.11.

5-Phenyldipyrromethane. The compound was synthesized according to the literature.[19] ^{1}H NMR (300 MHz, $CDCl_3$) δ 7.88 (br, 2H), 7.32–7.16 (m, 5H), 6.70–6.66 (m, 2H), 6.17–6.12 (m, 2H), 5.76–5.70 (m, 2H), 5.48 (s, 1H).

1,3,7,9-Tetramethyldipyrrin (1). Phosphorus oxychloride (4.59 g, 30 mmol) was slowly added to a degassed solution of 2,4-dimethylpyrrole (2.85 g, 30 mmol) and 3,5-dimethylpyrrole-

Table 1 Crystallographic data for the dipyrrinato Cu(I) complexes

Complex	**1b**	**2b**	**3a**	**4a**·MeOH	**5a**·MeOH	**6a**	**6b**·CH_2Cl_2	**7a**·Et_2O
Empirical formula	$C_{49}H_{43}CuN_2OP_2$	$C_{55}H_{47}CuN_2OP_2$	$C_{49}H_{43}Br_2CuN_2P_2$	$C_{52}H_{43}Cl_2CuN_2OP_2$	$C_{52}H_{43}Br_2CuN_2OP_2$	$C_{55}H_{44}CuF_5N_2P_2$	$C_{56}H_{44}Cl_2CuF_5N_2OP_2$	$C_{49}H_{44}CuN_2OP$
M_r	801.33	877.43	945.15	908.26	997.18	953.40	1052.31	697.25
Crystal system	Monoclinic	Triclinic	Triclinic	Triclinic	Triclinic	Triclinic	Triclinic	Triclinic
Space group	$P2_1/n$	$P\bar{1}$	$P\bar{1}$	$P\bar{1}$	$P\bar{1}$	$P\bar{1}$	$P\bar{1}$	$P\bar{1}$
a/Å	11.0197(15)	9.934(2)	11.0123(19)	11.4320(9)	11.374(3)	12.774(11)	12.7878(10)	12.4918(18)
b/Å	23.423(3)	12.945(3)	11.935(2)	11.5639(9)	11.686(3)	13.536(12)	13.0429(10)	14.252(2)
c/Å	15.859(2)	19.804(4)	17.701(3)	18.0545(15)	18.175(4)	14.094(12)	17.5091(13)	21.345(3)
α/°	90	105.232(4)	82.839(2)	80.6820(10)	80.042(3)	76.654(15)	87.8530(10)	90.005(2)
β/°	95.414(2)	94.756(4)	80.293(3)	85.9190(10)	85.355(4)	87.587(16)	72.3730(10)	86.958(2)
γ/°	90	109.758(4)	71.108(2)	75.1940(10)	75.425(4)	79.347(14)	61.4550(10)	89.993(3)
V/Å^3	4075.0(10)	2270.9(8)	2163.6(6)	2276.0(3)	2301.0(9)	2330(4)	2424.8(3)	3794.6(10)
Z	4	2	2	2	2	2	2	4
D_c/g cm^{-3}	1.306	1.283	1.451	1.279	1.393	1.359	1.441	1.221
μ/mm^{-1}	0.654	0.593	2.462	0.704	2.316	0.597	0.689	0.650
$2\theta_{max}$/°	52.14	52.22	52.10	52.04	52.06	52.14	52.06	52.26
No. reflns measd	22773	12927	12155	12891	12936	13174	13757	21357
No. reflns used (R_{int})	8024 (0.0697)	8797 (0.0515)	8278 (0.0171)	8764 (0.0151)	8817 (0.0195)	8950 (0.0306)	9369 (0.0305)	14623 (0.0438)
No. params	496	550	505	523	523	586	622	883
Final R [$I > 2\sigma(I)$], R_1, wR_2	0.0622, 0.1200	0.0766, 0.1336	0.0390, 0.0982	0.0382, 0.1015	0.0425, 0.0898	0.0656, 0.1292	0.0555, 0.1186	0.0603, 0.1495
R (all data), R_1, wR_2	0.1165, 0.1419	0.1535, 0.1670	0.0568, 0.1069	0.0487, 0.1072	0.0701, 0.0967	0.1000, 0.1481	0.0850, 0.1352	0.0748, 0.1562
GOF on F^2	1.010	0.996	1.028	1.008	1.002	1.054	0.992	0.995

2-carbaldehyde (3.69 g, 30 mmol) in n-hexane (30 ml) and CH_2Cl_2 (30 ml) at 0 °C with stirring over 15 min. A red precipitate formed was removed by filtration and washed with cold hexane. The precipitate was resolved in dichloromethane (50 ml) and washed with aqueous Na_2CO_3, water (100 ml × 3), dried over Na_2SO_4. The resulting solution was concentrated and then purified by flash column chromatography [inactivating Al_2O_3; hexane (containing 1% triethylamine)] to yield an orange crystalline solid (5.46 g, 91.0%). ^{1}H NMR (300 MHz, $CDCl_3$) δ 7.08 (br, 1H), 6.69 (s, 1H), 5.95 (s, 2H), 2.33 (s, 6H), 2.22 (s, 6H). ^{13}C NMR (151 MHz, $CDCl_3$) δ 152.84, 138.50, 137.56, 117.17, 116.58, 16.16, 11.39.

5-Phenyl-1,3,7,9-tetramethyldipyrrin (2). The same procedure as the preparation of **1** was used with (3,5-dimethylpyrrol-2-yl)-(phenyl)methanone as the starting material. Yield 6.51 g, 78.6%. ^{1}H NMR (300 MHz, $CDCl_3$) δ 13.21 (br, 1H), 7.42–7.13 (m, 5H), 5.88 (s, 2H), 2.34 (s, 6H), 1.29 (s, 6H). ^{13}C NMR (151 MHz, $CDCl_3$) δ 151.53, 140.40, 138.80, 138.07, 136.41, 129.24, 128.56, 128.14, 119.55, 16.03, 14.46.

2,8-Dibromo-1,3,7,9-tetramethyldipyrrin (3). Bromine (1.92 g, 12 mmol) in 20 ml chloroform was added dropwise to a solution of 1,3,7,9-tetramethyldipyrrin (**1**) (1.0 g, 5 mmol) in 15 ml chloroform over 10 min. The solution was stirred at room temperature for 3 h, and then washed with saturated aqueous $Na_2S_2O_3$ (100 ml × 3) and brine (100 ml × 3). The organic layer was dried over Na_2SO_4, evaporated under vacuum. The residue was purified by flash chromatography on Al_2O_3 with petroleum ether containing 1% triethylamine as eluent to yield **3** (1.59 g, 89%). ^{1}H NMR (600 MHz, $CDCl_3$) δ 11.04 (br, 1H), 6.66 (s, 1H), 2.33 (s, 6H), 2.15 (s, 6H); ^{13}C NMR (151 MHz, $CDCl_3$) δ 150.59, 136.18, 136.02, 117.01, 107.90, 14.89, 10.97.

1,9-Dichloro-5-phenyldipyrrin (4). A solution of *N*-chlorosuccinimide (NCS) (1.34 g, 10 mmol) in 20 ml THF was added to a solution of 5-phenyldipyrromethane (1.11 g, 5 mmol) in 50 ml dry THF at −78 °C. The reaction was stirred at −78 °C for 2 h and recovered to room temperature stirring 2 h. A solution of 5 mmol of DDQ in THF was added, and stirring was continued overnight. The resulting mixture was dissolved in dichloromethane (50 ml) and washed with water (100 ml × 3). The organic layer was dried over Na_2SO_4, concentrated and purified by flash chromatography on Al_2O_3 with petroleum ether to yield **4** (0.88 g, 61%). ^{1}H NMR (300 MHz, $CDCl_3$) δ 12.43 (br, 1H), 7.52–7.40 (m, 5H), 6.52 (d, J = 4.2 Hz, 2H), 6.25 (d, J = 4.2 Hz, 2H). ^{13}C NMR (151 MHz, $CDCl_3$) δ 141.78, 139.92, 138.45, 135.48, 130.79, 130.19, 129.32, 127.82, 116.93.

1,9-Dibromo-5-phenyldipyrrin (5). Ligand **5** was synthesized as for the preparation of **4** but with NBS as the starting material. Yield 1.30 g, 61%. ^{1}H NMR (600 MHz, $CDCl_3$) δ 12.47 (br, 1H), 7.50–7.38 (m, 5H), 6.46 (d, J = 4.2 Hz, 2H), 6.32 (d, J = 4.2 Hz, 2H). ^{13}C NMR (151 MHz, $CDCl_3$) δ 140.35, 139.39, 135.43, 130.74, 130.19, 129.53, 129.35, 127.85, 120.43.

5-Pentafluorophenyl-1,3,7,9-tetramethyldipyrrin (6). TFA (0.07 ml, 1 mmol) was added to a solution of 2,4-dimethylpyrrole (1.13 ml, 11 mmol) and pentafluorobenzaldehyde (0.62 ml, 5 mmol) in 30 ml absolute dichloromethane, and the solution was stirred at room temperature for 15 min. 1.36 g (6 mmol)

DDQ was added and then the mixture was stirred for 2 h and filtered. The filtrate was washed with brine (100 ml × 2), dried (Na_2SO_4), and concentrated under vacuum. The crude product was purified by flash column chromatography [Al_2O_3; hexane (containing 1% triethylamine)] to yield **6** (0.97 g, 53%) as a red solid: ^{1}H NMR (600 MHz, $CDCl_3$) δ 13.15 (br, 1H), 5.92 (s, 2H), 2.33 (s, 6H), 1.52 (s, 6H); ^{13}C NMR (151 MHz, $CDCl_3$) δ 153.23, 145.41, 143.77, 142.36, 140.67, 138.88, 138.29, 137.20, 135.88, 120.58, 119.41, 112.42, 16.08, 13.71; ^{19}F NMR (282 MHz, $CDCl_3$): δ −32.60 (dd, J = 22.9, 8.6 Hz, 2F), −45.36 (t, J = 20.8 Hz, 1F), −53.54 (dt, J = 22.8, 8.8 Hz, 2F).

1,5,9-Triphenyldipyrrin (7). Compound **7** was synthesized according to the literature.[20] 2-Phenylpyrrole (1.43 g, 10 mmol), benzoyl chloride (2.0 g, 7.4 mmol) and 1,2-dichloroethane (37 ml) were heated to reflux for 45 h, during which time the solution gradually acquired a purple hue. The reaction mixture was diluted with CH_2Cl_2 (50 ml) and washed with H_2O (50 ml), 1 M HCl (50 ml), 1 M NaOH (50 ml), and brine (50 ml), respectively. The organic portions were dried (Na_2SO_4), filtered and concentrated. The crude product was purified *via* flash chromatography on alumina using 30% CH_2Cl_2/hexanes as eluent to yield **7** as a dark purple solid (1.94 g, 49% yield); ^{1}H NMR (300 MHz, $CDCl_3$) δ 13.94 (br, 1H), 7.98 (d, J = 7.5 Hz, 4H), 7.62–7.44 (m, 11H), 6.89 (d, J = 4.2 Hz, 2H), 6.76 (d, J = 4.5 Hz, 2H); ^{13}C NMR (151 MHz, $CDCl_3$) δ 154.13, 142.02, 139.69, 137.17, 133.24, 133.00, 130.91, 129.95, 129.58, 129.02, 127.75, 126.20, 115.62.

Synthesis of complexes

Complex 1a. A degassed mixture of **1** (0.20 g, 1.0 mmol) and NaH (0.12 g, 5.0 mmol) were stirred in 10 ml newly evaporated THF for 2 h in flask A. CuI (0.19 g, 1.0 mmol) and triphenylphosphine (0.53 g, 2.0 mmol) were degassed and stirred in 10 ml THF for 2 h in flask B. The clear solution of sodic ligand in flask A after standing was transferred into the mixture of flask B. The reaction mass was stirred for 2 h, then the solvent was evaporated under vacuum to dryness. The solid residue was extracted with 10 ml absolute dichloromethane. The extract was filtered and transferred to an argon protected flask. 10 ml Methanol was layered above the resulting solution to afford yellow crystals of complex **1a** 0.69 g (87%). Mp 119 °C; ^{1}H NMR (300 MHz, $CDCl_3$): δ 7.44–7.31 (m, 30H), 6.99 (s, 1H), 5.96 (s, 2H), 2.29 (s, 12H); ^{13}C NMR (150 MHz, $CDCl_3$): δ 157.68, 141.07, 136.78, 135.36, 135.27, 133.91, 133.80, 129.34, 128.57, 128.52, 122.52, 116.63, 18.21, 11.75; ^{31}P NMR (242 MHz, $CDCl_3$): δ −0.18; Anal. Calc. for $C_{49}H_{45}CuN_2P_2$: C, 74.74; H, 5.76; N, 3.56. Found: C, 73.60; H, 5.95; N, 3.06%.

The following complexes were synthesized using the same procedure as the preparation of complex **1a**.

Complex 1b. 0.73 g (91%). Mp 175 °C; ^{1}H NMR (300 MHz, $CDCl_3$): δ 7.45–6.97 (m, 28H), 6.70 (s, 1H), 5.85 (s, 2H), 2.17 (s, 6H), 1.55 (s, 6H); ^{13}C NMR (150 MHz, $CDCl_3$): δ 158.99, 156.04, 140.13, 136.80, 135.11, 134.11, 130.58, 128.60, 128.24, 127.94, 124.29, 122.71, 119.91, 116.43, 18.88, 12.04; ^{31}P NMR (242 MHz, $CDCl_3$): δ −17.6; Anal. Calc. for $C_{49}H_{43}CuN_2OP_2$: C, 73.44; H, 5.41; N, 3.50. Found: C, 72.65; H, 5.38; N, 2.87%.

Complex 2a. 0.66 g (76%). Mp 137 °C; ^{1}H NMR (300 MHz, $CDCl_3$): δ 7.46–7.28 (m, 35H), 5.91 (s, 2H), 1.83 (s, 6H), 1.27 (s, 6H); ^{13}C NMR (75 MHz, $CDCl_3$): δ 156.84, 143.30, 133.94, 133.83, 129.86, 129.58, 129.21, 128.62, 128.57, 128.57, 128.32, 127.62, 120.28; ^{31}P NMR (242 MHz, $CDCl_3$): δ −1.16. Anal. Calc. for $C_{55}H_{49}CuN_2P_2$: C, 76.50; H, 5.72; N, 3.24. Found: C, 76.03; H, 5.40; N, 2.70%.

Complex 2b. 0.69 g (79%). Mp 159 °C; ^{1}H NMR (300 MHz, $CDCl_3$): δ 7.48–6.77 (m, 33H), 5.84 (s, 2H), 1.66 (s, 6H), 1.19 (s, 6H); ^{13}C NMR (150 HMz, $CDCl_3$): δ 155.30, 144.40, 142.25, 141.94, 136.54, 134.75, 134.09, 133.92, 130.40, 130.02, 129.20, 128.54, 127.86, 126.96, 123.99, 120.30, 119.40, 18.93, 15.88; ^{31}P NMR (242 MHz, $CDCl_3$): δ −16.6. Anal. Calc. for $C_{55}H_{47}CuN_2OP_2$: C, 75.28; H, 5.40; N, 3.19. Found: C, 74.30; H, 5.34; N, 2.92%.

Complex 3a. 0.79 g (84%). Mp 146 °C; ^{1}H NMR (300 MHz, $CDCl_3$): δ 7.32–7.14 (m, 30H), 6.97 (s, 1H), 2.24 (s, 6H), 1.74 (s, 6H); ^{13}C NMR (150 MHz, $CDCl_3$): δ 155.14, 138.30, 135.29, 135.19, 135.10, 133.86, 133.71, 129.44, 128.63, 128.58, 123.41, 106.66, 17.01, 11.41; ^{31}P NMR (242 MHz, $CDCl_3$): δ 0.19. Anal. Calc. for $C_{49}H_{43}Br_2CuN_2P_2$: C, 62.27; H, 4.59; N, 2.96. Found: C, 62.10; H, 4.40; N, 2.57%.

Complex 3b. 0.89 g (93%). Mp 147 °C; ^{1}H NMR (300 MHz, $CDCl_3$): δ 7.20–7.03 (m, 26H), 6.82 (d, J = 8.0 Hz, 2H), 6.68 (s, 1H) , 2.15 (s, 6H), 1.63 (s, 6H); ^{13}C NMR (150 MHz, $CDCl_3$): δ 158.56, 153.30, 135.14, 134.04, 133.90, 133.77, 133.71, 130.67, 128.73, 127.89, 127.58, 124.33, 123.36, 119.66, 106.06, 17.33, 11.36; ^{31}P NMR (242 MHz, $CDCl_3$): δ −17.0. Anal. Calc. for $C_{49}H_{41}Br_2CuN_2OP_2$: C, 61.36; H, 4.31; N, 2.92. Found: C, 61.27; H, 4.18; N, 2.45%.

Complex 4a. 0.71 g (81%). Mp 175 °C; ^{1}H NMR (300 MHz, $CDCl_3$) δ 7.50–7.28 (m, 35H), 6.45 (d, J = 4.2 Hz, 2H), 6.12 (d, J = 3.9 Hz, 2H), 3.49 (d, J = 5.1 Hz, 3H); ^{13}C NMR (150 MHz, $CDCl_3$): δ 159.06, 146.13, 146.02, 140.34, 139.90, 135.79, 134.73, 134.77, 133.92, 133.04, 131.29, 130.41, 128.44, 128.40, 127.66, 124.09, 119.90, 116.64; ^{31}P NMR (242 MHz, $CDCl_3$): δ 0.47. Anal. Calc. for $C_{51}H_{39}Cl_2CuN_2P_2{\cdot}CH_3OH$: C, 68.76; H, 4.77; N, 3.08. Found: C, 67.83; H, 4.39; N, 2.55%.

Complex 4b. 0.76 g (85%). Mp 139 °C; ^{1}H NMR (300 MHz, $CDCl_3$): δ 7.40–6.66 (m, 33H), 6.30 (d, J = 4.1 Hz, 2H), 6.03 (d, J = 4.1 Hz, 2H); ^{13}C NMR (75 MHz, $CDCl_3$): δ 158.46, 145.63, 145.12, 139.48, 138.26, 134.00, 133.94, 133.89, 133.50, 131.99, 130.60, 130.44, 128.55, 128.29, 127.79, 127.45, 126.62, 123.93, 119.42, 115.14; ^{31}P NMR (121 MHz, $CDCl_3$): δ −14.9. Anal. Calc. for $C_{51}H_{37}Cl_2CuN_2OP_2$: C, 68.81; H, 4.19; N, 3.15. Found: C, 67.53; H, 4.35; N, 2.48%.

Complex 5a. 0.85 g (88%). Mp 147 °C; ^{1}H NMR (300 MHz, $CDCl_3$): δ 7.48–7.28 (m, 35H), 6.41 (d, J = 4.2 Hz, 2H), 6.26 (d, J = 4.2 Hz, 2H), 3.49 (d, J = 5.1 Hz, 3H); ^{13}C NMR (150 MHz, $CDCl_3$): δ 146.14, 140.48, 138.81, 137.18, 134.86, 134.55, 134.35, 133.30, 132.43, 131.11, 129.85, 128.89, 128.77, 128.58, 127.42, 119.73; ^{31}P NMR (242 MHz, $CDCl_3$): δ −0.005; Anal. Calc. for $C_{51}H_{39}Br_2CuN_2P_2{\cdot}CH_3OH$: C, 62.63; H, 4.35. N, 2.81. Found: C, 62.62; H, 4.34; N, 2.44%.

Complex 5b. 0.82 g (84%). Mp 150 °C; ^{1}H NMR (300 MHz, $CDCl_3$): δ 7.37–7.00 (m, 31H), 6.79–6.78 (m, 2H), 6.22 (d, J = 4.1 Hz, 2H), 6.12 (d, J = 4.1 Hz, 2H); ^{13}C NMR (75 MHz, $CDCl_3$): δ 140.58, 139.81, 135.75, 134.73, 134.57, 134.46, 134.36, 134.19, 132.53, 130.86, 128.13, 127.02, 124.31, 119.84, 119.37; ^{31}P NMR (121 MHz, $CDCl_3$): δ −17.91. Anal. Calc. for $C_{51}H_{37}Br_2CuN_2OP_2$: C, 62.56; H, 3.81; N, 2.86. Found: C, 61.38; H, 4.12; N, 2.19%.

Complex 6a. 0.70 g (74%). Mp 132 °C; ^{1}H NMR (300 MHz, $CDCl_3$): δ 7.44–7.34 (m, 30H), 5.95 (s, 2H), 1.82 (s, 6H), 1.52 (s, 6H); ^{13}C NMR (75 MHz, $CDCl_3$): δ 158.77, 140.77, 135.34, 135.26, 135.16, 133.88, 133.77, 129.40, 128.64, 128.59, 121.33, 18.74, 15.10; ^{19}F NMR (282 MHz, $CDCl_3$) δ −33.08 (dd, J = 24.2, 8.2 Hz, 2F), −48.40 (t, J = 20.8 Hz, 1F), −55.40 (td, J = 23.1, 8.0 Hz, 2F); ^{31}P NMR (121 MHz, $CDCl_3$): δ 0.87. Anal. Calc. for $C_{55}H_{44}CuF_5N_2P_2$: C, 69.28; H, 4.65; N, 2.94. Found: C, 67.95; H, 4.63; N, 2.32%.

Complex 6b. 0.80 g (83%). Mp 131 °C; ^{1}H NMR (300 MHz, $CDCl_3$): δ 7.20–6.89 (m, 28H), 5.84 (s, 2H), 1.53 (s, 6H), 1.47 (s, 6H); ^{13}C NMR (75 MHz, $CDCl_3$): δ 158.68, 157.16, 147.03, 139.98, 136.72, 135.69, 134.88, 134.55, 134.34, 134.24, 130.84, 128.99, 128.26, 125.18, 124.54, 121.77, 119.72, 19.16, 15.63; ^{19}F NMR (282 MHz, $CDCl_3$) δ −32.75 (dd, J = 23.3, 8.7 Hz, 2F), −47.03 (t, J = 21.0 Hz, 1F), −54.50 (t, J = 18.5, 8.0 Hz, 2F); ^{31}P NMR (121 MHz, $CDCl_3$): δ −16.24. Anal. Calc. for $C_{55}H_{42}CuF_5N_2OP_2{\cdot}CH_2Cl_2$: C, 63.91; H, 4.21; N, 2.66. Found: C, 63.23; H, 4.31; N, 2.13%.

Complex 7a. 0.52 g (75%). Mp 105 °C; ^{1}H NMR (300 MHz, $CDCl_3$): δ 7.83–7.79 (m, 4H), 7.62–7.59 (m, 2H), 7.45–7.42 (m, 2H), 7.29–7.24 (m, 6H), 7.16–7.11 (m, 6H), 6.95–6.81 (m, 10H), 6.78 (d, J = 4.2 Hz, 2H), 6.71 (d, J = 4.1 Hz, 2H), 3.48 (q, J = 7.0 Hz, 4H), 1.21 (t, J = 7.0 Hz, 6H); ^{13}C NMR (75 MHz, $CDCl_3$): δ 133.86, 133.67, 132.72, 131.50, 129.74, 128.68, 128.55, 128.27, 127.99, 127.66, 127.27, 116.57; ^{31}P NMR (121 MHz, $CDCl_3$): δ −15.72. Anal. Calc. for $C_{45}H_{34}CuN_2P{\cdot}CH_3CH_2OCH_2CH_3$: C, 76.29; H, 5.75; N, 3.63. Found: C, 75.93; H, 5.39; N, 3.74%.

Results and discussion

Synthesis of ligands

All of the dipyrrins employed in this work are symmetrical structures containing substituents at the 1,9-positions. A major consideration is to inhibit the geometry torsion through the steric hindrance effect of these groups, because the change between tetrahedral and square-planar geometries in Cu(I) complexes always take place from the ground to excited states as a result of MLCT.[1] The basic dipyrrins were synthesized according to the literature as previously reported.[8b] For example, ligands **1** and **2** were prepared by the condensation of 2,4-dimethylpyrrole and the corresponding aldehyde or ketone in presence of phosphorus oxychloride ($POCl_3$) in good yields, while **6** was prepared *via* oxidation after the reactions of 2-substituted pyrrole and benzoyl chloride (Scheme 1). Attempts to synthesize **2** *via* one-pot condensation of 2,4-dimethylpyrrole and the aldehyde or acyl chloride in the presence of acid just gave low yields (27% and 18%).

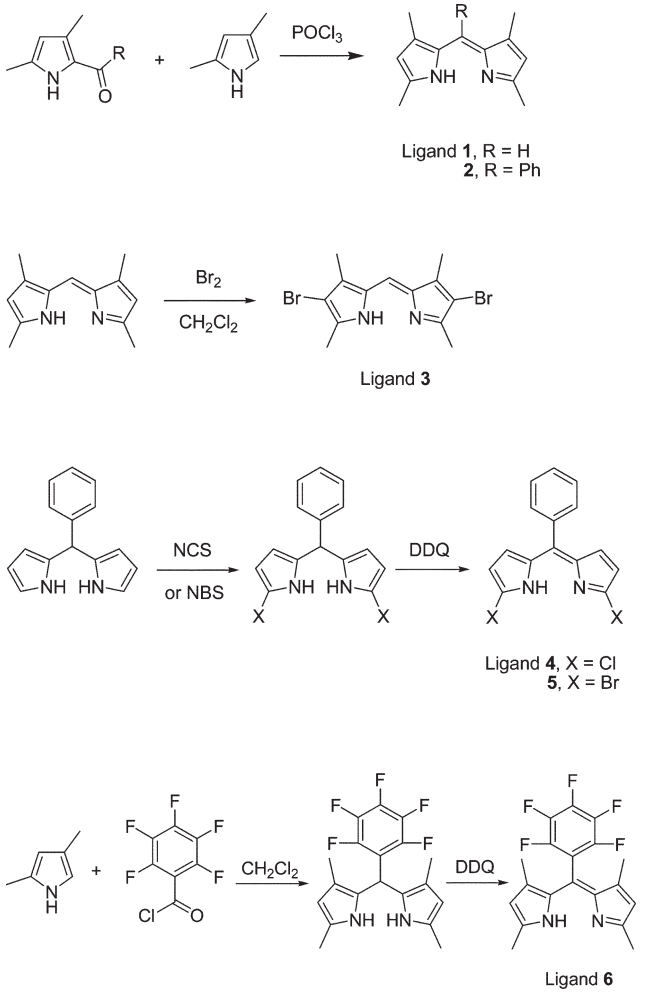

Scheme 1 The synthesis route of ligands.

Ligand **3** was obtained by the bromination from compound **1** using bromine in higher yield than using *N*-bromosuccinimide (NBS). Dipyrrins **4** and **5** were isolated *via* the DDQ oxidation of their corresponding dipyrromethane precursor prepared by the bromination of 5-phenyldipyrrin using NCS or NBS. It is interesting that the regioselective halogenations of dipyrromethane only take place at 1,9-positions when using NCS and NBS. In contrast, the bromination first take place at 2,8-positions if using BODIPY and bromine as the starting materials according to recently reported results.[21] Another aim of introducing halogen atoms is to investigate the influence on the electronic structures of the Cu(I) complexes.

Synthesis of complexes

The chemical structures of the complexes are shown in Scheme 2. All ligands were first deprotonated using NaH in THF to give the sodium salts of dipyrrin. After standing, the solution of the sodic ligand was added to the mixture of cuprous iodide and phosphine aged in advance so as to easily obtain the neutral dipyrrinato cuprous complexes *via* the elimination of NaI. The use of stronger bases such as n-butyllithium, however, causes

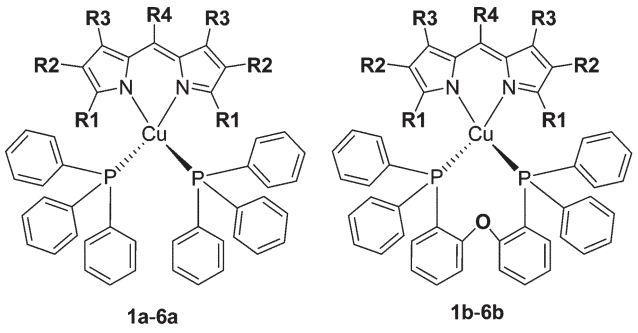

1a	R1 = CH_3	R2 = H	R3 = CH_3	R4 = H
2a	R1 = CH_3	R2 = H	R3 = CH_3	R4 = Ph
3a	R1 = CH_3	R2 = Br	R3 = CH_3	R4 = H
4a	R1 = Cl	R2 = H	R3 = H	R4 = Ph
5a	R1 = Br	R2 = H	R3 = H	R4 = Ph
6a	R1 = CH_3	R2 = H	R3 = CH_3	R4 = pF-Ph
1b	R1 = CH_3	R2 = H	R3 = CH_3	R4 = H
2b	R1 = CH_3	R2 = H	R3 = CH_3	R4 = Ph
3b	R1 = CH_3	R2 = Br	R3 = CH_3	R4 = H
4b	R1 = Cl	R2 = H	R3 = H	R4 = Ph
5b	R1 = Br	R2 = H	R3 = H	R4 = Ph
6b	R1 = CH_3	R2 = H	R3 = CH_3	R4 = pF-Ph

pF-Ph = pentafluorophenyl

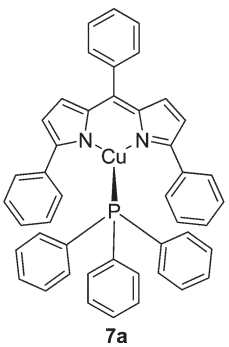

Scheme 2 The molecular structures of the Cu(I) complexes.

side reactions and isolation problems of the complexes. The preparation reactions were easily monitored by the quenching of the bright green fluorescence of the sodium salt of the ligand and the color change of the solution from orange–red to brown. All complexes were further purified *via* recrystallization using the slow diffusion of methanol into CH_2Cl_2 solutions to lead to metallic lustre crystals. The complexes in solution oxidize readily to form Cu(II) compounds accompanied by a color change of dark green, but the crystals are relative stable on exposure to air.

The identity of the complexes were confirmed by multinuclear NMR spectroscopy and elemental analyses. The resonance signals of active proton at 12 ppm for free ligands are absent in the complexes. For other proton and ^{13}C signals, only slight changes were found, indicating that the electronic structures of the dipyrrins remain relatively unperturbed upon coordination. However, the ^{31}P signals occur over a large shift range as a result of the coordination effect. Only one ^{31}P signal was observed for all the Cu(I) complexes due to the symmetrical ligand structure.

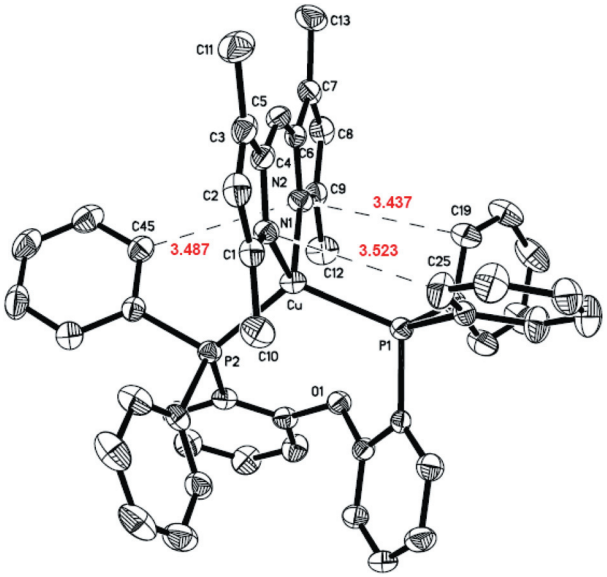

Fig. 1 The molecular structure of **1b**. The intramolecular edge-to-face π–π interactions between dipyrrin and phenyl rings are indicated (C19–N2 3.437 Å, C45–N2 3.487 Å, C25–N1 3.523 Å). Hydrogen atoms have been omitted for clarity.

The ^{31}P resonance of complex **7a** is at $\delta = -15.73$ ppm, which is at higher field relative to the free PPh_3 ligand ($\delta = -4.60$ ppm), while the ^{31}P signals of other complexes with PPh_3 as the ancillary ligand ($\delta = -1.18$–0.47 ppm) are shifted down field. The ^{31}P signals of complex **1b–6b** ($\delta = -14.9$–17.9 ppm) are near to those of the free DPEphos ligand ($\delta = -16.40$ ppm), which are the similar to those observed in the literatures.[5f,6a]

Crystal structural investigations

Single-crystal X-ray diffraction study of eight complexes was carried out to further confirm the structures of these molecules. The molecular structures of complexes **1b**, **2b**, **3a**, **4a**, **5a**, **6a**, **6b** and **7a** are shown in Fig. 1–8. Selected bond distances and angles of complexes are reported and compared in Table 2. Except for complex **7a**, which is tricoordinated in pyramidal coordination geometry owing to serious steric hindrance, the other complexes all display a pseudo-tetrahedral coordination environment. The **a** series complexes always tend towards an ideal tetrahedron due to the symmetrical structural ligand and monodentate PPh_3. In contrast, the **b** series often adopt the more distorted tetrahedral geometries due to the restricted bite angle of the bidentate ligand of DPEphos.[5f,7,22] The dihedral angles (φ) between the N–C_{meso}–N and P–Cu–P planes for the complexes are in the normal range of 85.4–89.0°.

The N–Cu bond lengths are obviously shorter than those of the cationic [Cu(phen)(PP)]$^+$ complexes (phen = phenanthroline, PP = one bidentate phosphine ligand or two monodentate phosphine ligands),[3] and similar to those in analogues.[6] Most of the P–Cu bond lengths are longer than those of the cationic [Cu(phen)(PP)]$^+$ complexes.[3] The N–Cu–N bond angles for all complexes are larger than those of the cationic Cu(I) complexes. These data indicate that there is a stronger link in the neutral

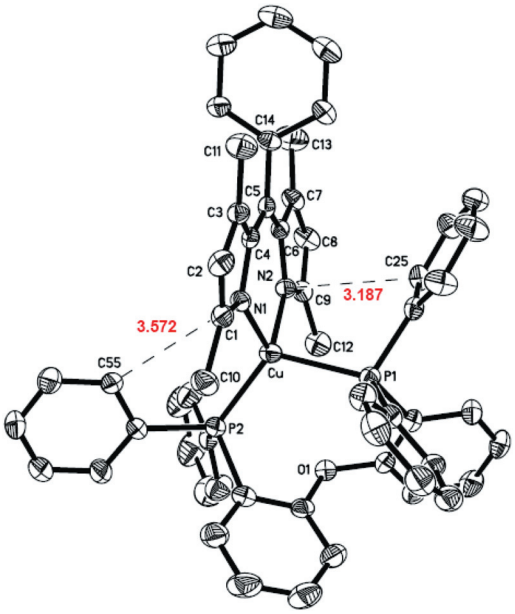

Fig. 2 The molecular structure of **2b**. The intramolecular π–π interactions between dipyrrin and phenyl rings are indicated (C25–N2 3.187 Å (face-to-face) and C55–N1 3.572 Å (edge-to-face)). Hydrogen atoms have been omitted for clarity.

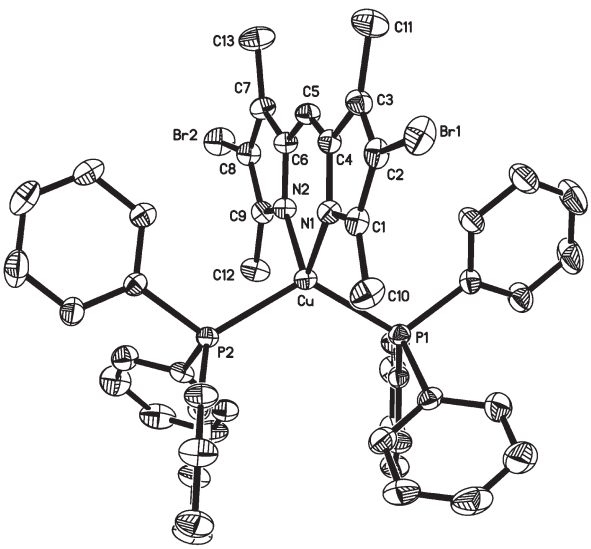

Fig. 3 The molecular structure of **3a**. Hydrogen atoms have been omitted for clarity.

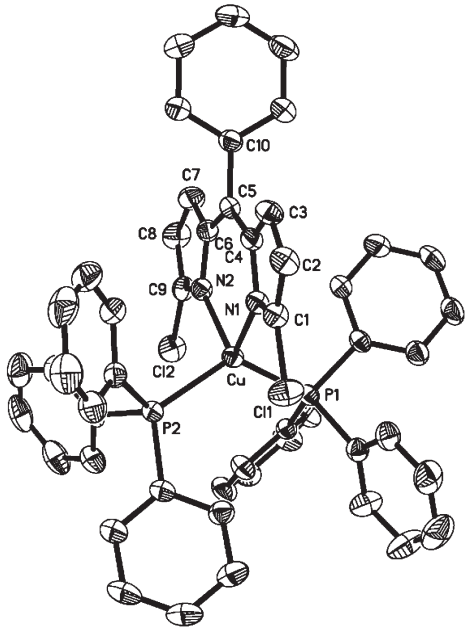

Fig. 4 The molecular structure of **4a**. Hydrogen atoms have been omitted for clarity.

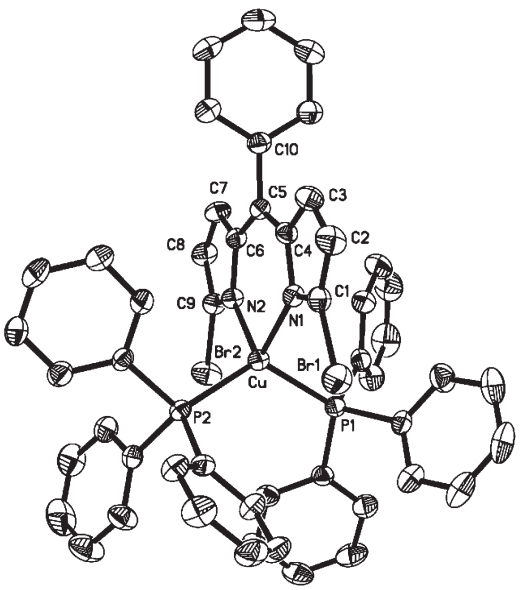

Fig. 5 The molecular structure of **5a**. Hydrogen atoms have been omitted for clarity.

complexes than the cationic complexes between the NN ligand and the central Cu(I) atom. The $C_{pyrrole}$–C_{meso}–$C_{pyrrole}$ bond angles of the ligand backbone in these dipyrrinato Cu(I) complexes are expanded compared to those (119.66 and 121.34°) in BODIPYs,[23] which results in a clear twist of two pyrrole rings rather than the expected coplanar conjugate system. The characteristic has also been observed for other luminescent transition-metal complexes containing an analogous ligand.[14]

Most of the Cu(I) atoms of the complexes are nearly coplanar with the dipyrrin ligand. The sum internal angles of the six-membered metal chelating ring (CuNCCCN) are nearly 720° for a coplanar hexagon. For complex **6b**, however, the sum of internal angles is 694.84° and Cu atom is pulled out of the dipyrrin plane by 0.98 Å, and meanwhile induce a smallest N–Cu–N bond angle [88.63(11)°]. A similar case is also observed in the complex **7a** with Cu 0.55 and 0.56 Å out of dipyrrin plane because of the steric hindrance of α-phenyls. In the **b** series complexes, intramolecular π–π interactions between dipyrrin and phenyl rings are found while DPEphos acts as the ancillary ligand (see Fig. 1, 2 and 7). In complexes **1b** and **6b**, only edge-

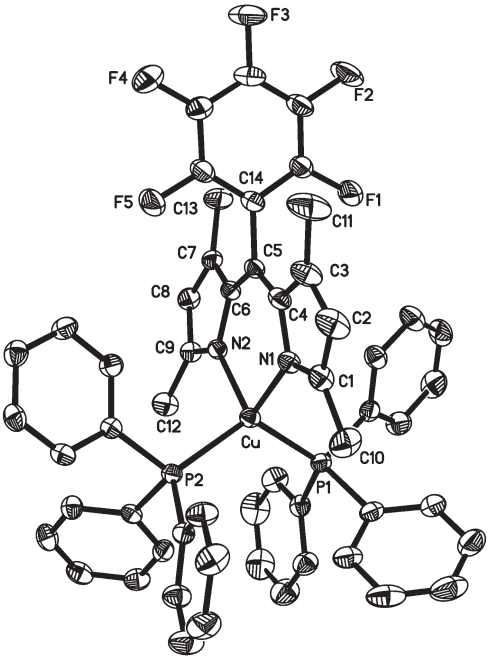

Fig. 6 The molecular structure of **6a**. Hydrogen atoms have been omitted for clarity.

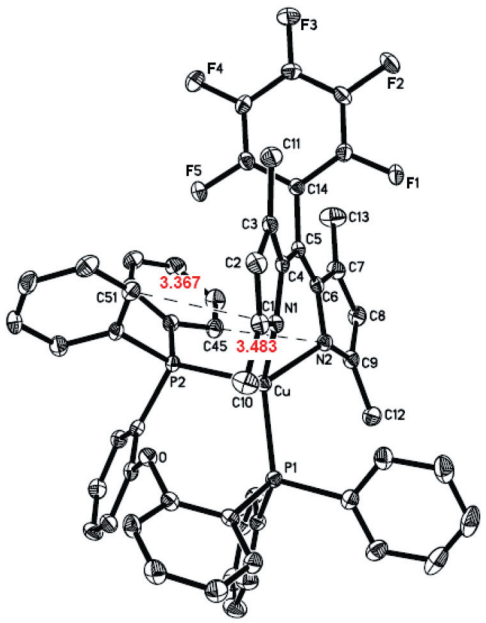

Fig. 7 The molecular structure of **6b**. The intramolecular edge-to-face π–π interactions between dipyrrin and phenyl rings are indicated (C51–N1 3.367 Å and C45–N2 3.483 Å). The solvent and hydrogen atoms have been omitted for clarity.

to-face interactions exist at 3.19–3.57 Å. In **2b**, there are near parallels between dipyrrin plane and a phenyl ring with face-to-face interaction. These differences result in the differently distorted extent of the tetrahedron around Cu(I) atom, in which the complex **6b** exhibits the most distorted tetrahedral geometry due to the presence of the interaction only at single-side.

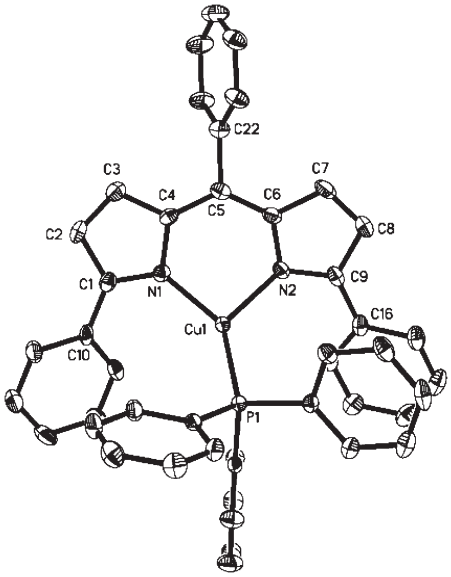

Fig. 8 The molecular structure of **7a**. Hydrogen atoms have been omitted for clarity.

Photophysical properties

UV-Vis spectra of the complexes were recorded in dichloromethane as shown in Fig. 9, and the resulting data are summarized in Table 3. The complexes all show the similar absorption features to those of BODIPYs and aza-BODIPY dyes including an analogous Cu(I) complex with an azadipyrromethene ligand.[24] The absorption maxima appearing at 495 nm is assigned to the 0–0 band of a strong S0–S1 transition within the dipyrrinato anion, while its shoulder at short wavelength (~460 nm) is attributed to the 0–1 vibrational band of the same transition.[25] The weak absorption bands between 250–400 nm are due to the S0–S2 transition of the dipyrrinato anion, which may be contain an MLCT contribution since the absorption band of heteroleptic $[Cu(phen)(PP)]^+$ complexes generally occurs in the range of 300–450 nm.[3a] Another maximum absorption at ~230 nm are assigned to the π–π* absorption of phenyl groups, while its shoulder at ~260 nm are due to proximal phenyl group participation in the ligand-centered transitions. The maximum of the S0–S1 transition within the dipyrrinato anion exhibits a considerable variation with the various substitution patterns. Complexes **6a** and **6b** with strong electron withdrawing pentafluorophenyl at *meso*-carbon red-shift their S0–S1 transition to 512 and 510.5 nm, respectively. The maximum absorptions of **3a**, **3b**, **5a** and **5b** are located at 506, 504.5, 499 and 500 nm, respectively, which indicates that bromine substituent at 2,8-positions is more efficient than at 1,9-positions (α-positions) in red-shifting the maximum of the S0–S1 transition. The chlorine atom is somewhat weaker than bromine atom as auxochrome in red-shifting spectra according to the maximum absorption of **4a** and **4b** (493 and 496 nm). An exception is the complex **7a**, for which the maximum absorption red-shifts ~60 nm relative to the simple substituted complexes **1a** and **1b** (487 and 484 nm), but blue-shifts ~50 nm compared to the same three-coordinate azadipyrromethene Cu(I) complex.[24c]

Table 2 Selected bond distances (Å) and angles (°) for the dipyrrinato Cu(I) complexes

Complex	1b	2b	3a	4a	5a	6a	6b	7a
Cu–N(2)	2.028(3)	1.996(4)	2.072(2)	2.0519(17)	2.061(2)	2.038(3)	2.068(3)	1.994(3) [1.994(3)]
Cu–N(1)	2.036(3)	2.003(4)	2.067(2)	2.0414(16)	2.059(2)	2.050(3)	2.020(3)	1.966(3) [1.962(3)]
Cu–P(2)	2.3078(12)	2.2383(15)	2.3075(8)	2.2765(6)	2.2765(10)	2.287(2)	2.3555(10)	n/a
Cu–P(1)	2.3061(11)	2.3780(16)	2.2976(9)	2.2696(6)	2.2882(10)	2.305(2)	2.2424(10)	2.1708(10) [2.1650(10)]
N(2)–Cu–N(1)	97.35(13)	95.17(16)	95.05(9)	92.45(7)	92.57(10)	92.49(14)	88.63(11)	95.43(13) [95.83(13)]
N(2)–Cu–P(2)	110.82(9)	119.70(12)	106.18(7)	107.83(5)	114.41(7)	109.39(9)	111.28(8)	n/a
N(1)–Cu–P(2)	112.74(9)	118.33(12)	113.55(7)	105.69(5)	108.77(7)	112.20(10)	104.82(8)	n/a
N(2)–Cu–P(1)	106.58(10)	100.56(12)	112.36(7)	108.27(5)	105.29(7)	109.88(10)	117.03(8)	138.15(10) [133.58(10)]
N(1)–Cu–P(1)	111.33(9)	103.60(12)	107.29(7)	113.85(5)	108.55(7)	110.10(11)	123.25(8)	122.37(10) [127.55(9)]
P(2)–Cu–P(1)	116.20(4)	115.95(6)	119.71(3)	124.06(2)	122.95(3)	119.46(5)	109.89(4)	n/a
$C_{pyrrole}$–C_{meso}–$C_{pyrrole}$	132.2(4)	129.4(5)	131.3(3)	128.0(2)	128.3(3)	130.1(3)	128.4(3)	127.8(4) [127.7(4)]
Cu–(N–C_{meso}–N)/Å	0.1068	0.2087	0.0123	0.1234	0.1199	0.0173	0.9758	0.5536 (0.5625)
P(1)–(N–C_{meso}–N)/Å	2.1954	2.5547	2.0053	2.1537	1.8653	1.9727	0.8397	1.9521 (1.9260)
P(2)–(N–C_{meso}–N)/Å	1.6923	1.0790	1.9639	1.8548	2.1376	1.9925	3.2299	n/a
φ(N–C_{meso}–N/P–Cu–P)/°	88.5	88.0	85.4	87.1	86.7	89.0	86.0	n/a
$\Sigma_{metallacycle}$ (CuNCCCN)/°	719.56	717.51	719.39	719.50	719.64	716.87	694.83	710.33 (711.03)

As shown in Fig. 10, all complexes show a similar emission band to BODIPY compounds with narrow Stokes' shift, absorption and emission 'mirror image' relationship and a nanosecond-order lifetime. The emission of complex **7a** red-shifts to the orange–red region with the maximum at 595 nm. The emission patterns are not affected by the ancillary phosphine ligands with nearly identical maxima emission wavelength between the pairs of complexes **a** and **b**. This is different from the classical $[Cu(NN)(PP)]^+$ complexes often accompanying 10 nm variation.[3] The perfect mirror symmetry (see ESI, Fig. S1–S12‡) indicates that the main absorption band at ~500 nm corresponds to the S0–S1 transition. The quantum yields of these complexes in CH_2Cl_2 were measured and are given in Table 3. The values of the complexes are similar with either PPh_3 or DPEphos as ancillary ligand, however, they are obviously lower than those of the BODIPY dyes due to the twisted structures of dipyrrinato anion upon coordination (see Crystal structural investigations section). A reasonable explanation is that the vibration of the dipyrrin skeleton substantially increases the probability of non-radiative transition due to geometric distortion.[14] The results described above suggest that the emissive properties of these Cu (I) complexes fundamentally depend on the structure of the dipyrrin ligands.

The small Stokes' shift and nanosecond-order lifetimes in all complexes are consistent with singlet fluorescence. Similar emissive behaviors to BODIPYs also indicate that the emission of these complexes should be from the dipyrrin-centered intraligand charge transition (ILCT). To further verify the assignment, boron difluoride compound (**1**)BF_2 was synthesized by the reaction of ligand **1** and $BF_3{\cdot}OEt_2$ according to the literature.[1] The absorption and emission spectra of the boron compound and free ligand in CH_2Cl_2 are presented in Fig. S14 and S15 (ESI‡). The compound exhibited maximum absorption and emission peaks at 506 and 522 nm in CH_2Cl_2, respectively, with minor variation compared to the literature (505 and 516 nm in EtOH).[1] Obviously, these peaks are red-shifted relative to those of the complexes **1a** and **1b**. However, this is reasonable because of better coplanarity, indicating the smaller energy difference,

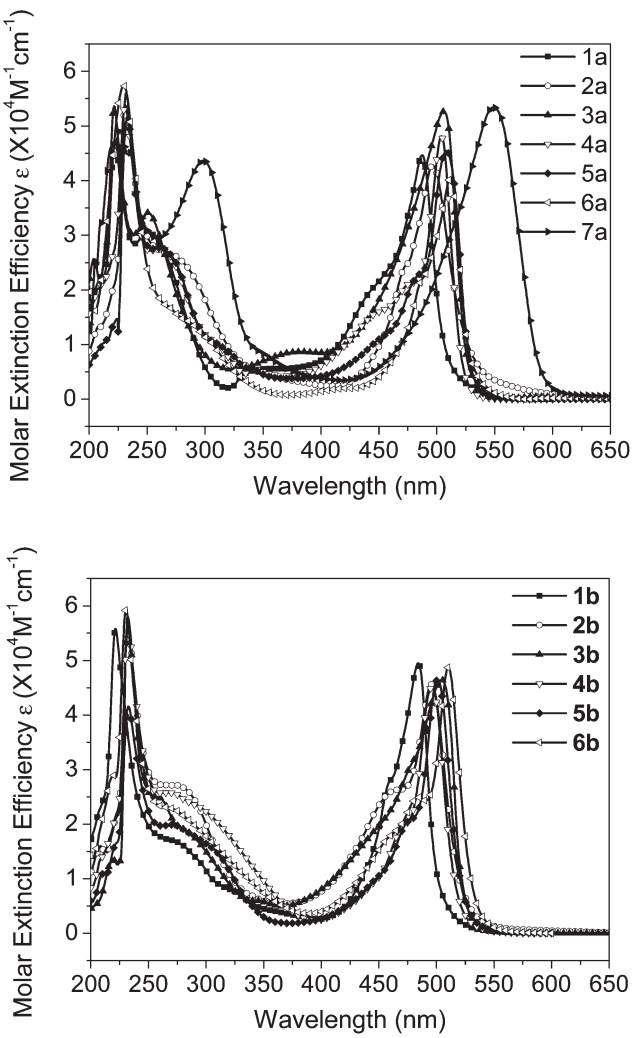

Fig. 9 Absorption spectra of the complexes **1a–7a** (top) and **1b–6b** (bottom) in CH_2Cl_2 at room temperature.

Table 3 Photophysical properties of the complexes[a]

	λ_{abs}^{max}/nm ($10^{-3}\varepsilon$/M^{-1} cm^{-1})	$\Delta\lambda_{Stokes}$/nm	λ_{em}^{max}/nm	τ/ns	Φ (%)
1a	487 (44.7), 450 (21.5), 252 (30.8), 231 (47.2)	9.0	496	5.9	0.4
1b	484 (49.5), 460 (27.9), 280 (16.3), 231 (55.8)	11.0	495	6.2	0.9
2a	496 (42.1), 457 (33.2), 274 (26.3), 230 (56.1)	14.0	510	5.5	0.1
2b	496 (45.5), 465 (26.3), 273 (27.0), 230 (58.0)	13.0	509	5.4	0.1
3a	506 (46.7), 251 (34.5), 230 (53.6)	9.0	515	5.3	3.3
3b	504.5 (46.4), 261 (24.6), 230 (58.1)	11.5	516	5.6	4.0
4a	493 (48.1), 463.5 (21.5), 362 (27.7), 231 (53.8)	12.0	505	7.5	0.3
4b	496 (45.0), 471 (19.7), 267 (25.8), 232 (56.1)	9.0	505	5.8	0.6
5a	499 (45.4), 475.5 (22.9), 260 (27.5), 230 (51.5)	10.0	509	5.9	0.1
5b	500 (46.5), 477.5 (21.2), 290 (14.0), 230 (52.1)	9.0	509	6.0	0.6
6a	512 (40.5), 488 (22.4), 286 (14.5), 230 (57.4)	33.0	545	7.0	0.1
6b	510.5 (48.7), 484 (24.9), 272 (22.4), 232 (59.5)	33.5	544	6.8	0.1
7a	549 (53.4), 298 (43.7), 224 (48.8)	46.0	595	7.6	0.2

[a] [conc.] ≈ 5×10^{-6} M in dichloromethane.

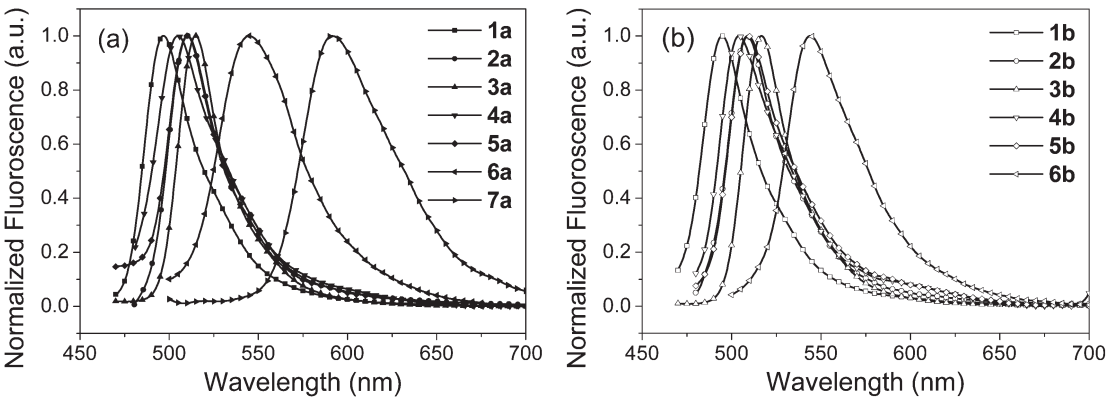

Fig. 10 Room-temperature emission spectra for complexes **1a–7a** (a) and **1b–6b** (b) in degassed CH_2Cl_2 at ~5×10^{-6} M.

between the two pyrrolic rings in the compound (**1**)BF_2.[23] In addition, the free ligand even shows red-shifted emission at 507 nm in comparison with the corresponding Cu(I) complexes. Therefore, these direct experimental data supports the above postulate. This is different from the traditional 1,10-phenanthroline cuprous cationic complexes, in which the main emission is usually assigned to MLCT.[3,26] However, similar fluorescent behaviors have also been found in the Pt(II) complexes with ligands showing extended conjugation.[27] The increased conjugation within the electron-rich dipyrrinato anion decreases the π–π* transition energy barrier, and simultaneously weakens the interaction between the dipyrrin ligand and Cu(I) atom, which makes the π–π* transition more favorable. The weak interaction prevents the effective mixing of π orbitals of dipyrrin and 3d orbitals of Cu(I) atom due to the bigger gap of the energy level (see Electrochemistry part), and restrains the spin-forbidden d–π* transition.[27]

To further understand the photophysics properties of the neutral dipyrrinato cuprous compounds, density functional theory (DFT) calculation was performed using the B3LYP functional with the Lanl2DZ basis set for Cu and Br, and 6-311++g** for the other atoms. The geometries for DFT calculation were from the X-ray structure results. As shown in Fig. 11, the highest occupied molecular orbitals (HOMOs) and lowest unoccupied molecular orbitals (LUMOs) of the dipyrrinato cuprous complexes are all distributed on the dipyrrin π and π* orbitals, which is consistent with the investigation in the BODIPY system.[28] No contribution from the central Cu(I) atom illustrates that there is no MLCT transition in the absorption spectra of these complexes and the emission should be assigned to ILCT within the dipyrrinato anion.

Electrochemistry

The electrochemical properties of the complexes and ligands were investigated using cyclic voltammetry and all data are summarized in Table 4. Compared to the voltammetric behavior of free ligands, a novel and lower oxidation peak is observed at potentials ranging from 0.56 to 1.02 V and attributed to the oxidation of Cu(I) to Cu(II). Facile oxidations of the complexes are reasonable because the electron-donating effect of dipyrrinato anion significantly increases the electron density on the central Cu(I) atom. The oxidation potentials of the ligands only display a small variation, but their reduction waves distinctly shift to more cathodic values according to substituents with the potentials ranging from −1.24 to −1.72 V. The reduction potentials of **1a**, **1b** and **2b** are not found in the electrochemical window.

The redox potentials of the complexes and the free ligands are affected by the electronic character and the substitution position

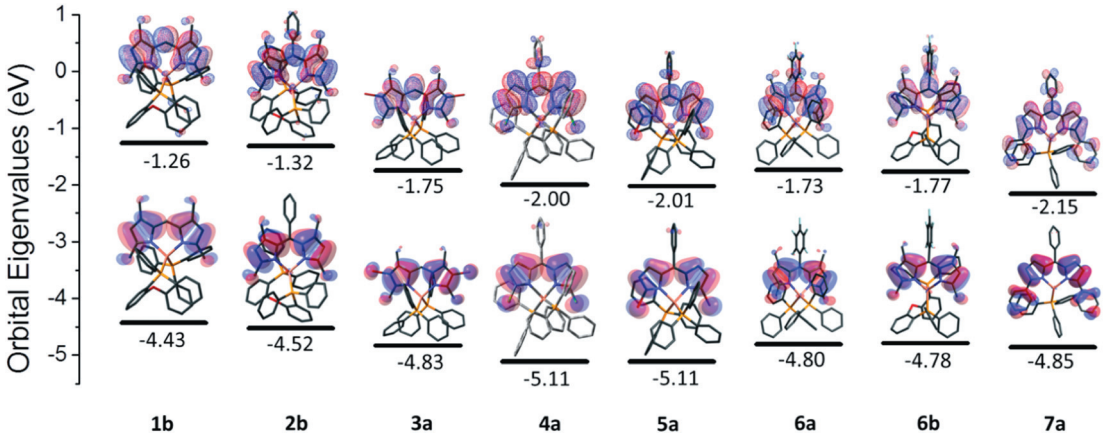

Fig. 11 Qualitative orbital energy diagram illustrating the HOMO (transparent) and LUMO (mesh) orbitals of **1b**, **2b**, **3a**, **4a**, **5a**, **6a**, **6b** and **7a**. All values reported in eV.

Table 4 Electrochemical data (E/V) for the complexes and their ligands in dichloromethane (scan rate 50 mV s^{-1})

	$E_{1/2}^{Ox}$	$E_{1/2}^{Red}$		$E_{1/2}^{Ox}$	$E_{1/2}^{Red}$		$E_{1/2}^{Ox}$	$E_{1/2}^{Red}$
1	0.82, 1.53	−1.63	**1a**	0.52, 0.73, 1.30	n/a	**1b**	0.36, 0.75	n/a
2	0.86, 1.46	−1.57	**2a**	0.64, 0.99, 1.33	−1.69	**2b**	0.38, 0.65, 1.46	n/a
3	1.01	−1.34	**3a**	0.70, 0.96, 1.34	−1.55	**3b**	0.59, 1.26, 1.69	−1.69
4	1.33	−1.09	**4a**	0.86, 1.21	−1.33	**4b**	0.82, 1.18, 1.71	−1.51
5	1.35	−1.06	**5a**	1.02, 1.39	−1.24	**5b**	0.90, 1.35	−1.26
6	1.02	−1.37	**6a**	0.64, 0.86, 1.32	−1.59	**6b**	0.54, 1.54	−1.72
7	1.02, 1.46	−1.11	**7a**	0.72, 1.34, 1.49	−1.42			

of the substituents. Complexes **5a** with α-bromine atoms exhibit the most anodic Cu(I)–Cu(II) oxidation potential (1.02 V) in this series of complexes, while its free ligand **5** also exhibit the most anodic first oxidation potential (1.35 V) in the ligands. The analogous complex **4a** (0.86 V) and its free ligand **4** (1.33 V) with α-chlorine atoms show relatively anodic oxidation waves. However, the complexes **3a** (0.70 V) and the free ligand 3 (1.01 V) with bromine atom substituents at 2,8-positions on dipyrrin are not as anodic as their analogues with halogen substituents at 1,9-position. The increased conjugation of dipyrrin reduces the HOMO–LUMO gap of the ligand and corresponding complex, and thus complex **7a** (2.14 V) and its free ligand **7** (2.13 V) have the lowest HOMO–LUMO gap. The cuprous complexes with stronger electron-donor DPEphos cathodically shift the oxidation potentials ~0.1 V compared to those of complexes with PPh_3 as ancillary ligand, and meanwhile, DPEphos shifts the reduction potentials of the dipyrrinato anion cathodically somewhat as well. In general, the **b** series complexes display quasi-reversible and multiple oxidation peaks attributed to multiple electron-transfer originating from the Cu(I) center and phosphine ligand, implying that these complexes have higher electrochemical stability due to the chelating effect of the DPEphos ligand.[29] Complexes **4a** and **4b**, with the more negative chlorine atoms on dipyrrin, all show a reversible reduction process. Due to the decreased conjugation within the dipyrrinato anion resulting from the steric hindrance upon coordination, complex **7a** exhibits quasi-reversible reduction while the reduction process of ligand **7** is reversible at −1.11 V.

The relatively low oxidation potentials of Cu(I) ion indicate that its d orbital energy levels are high. In contrast, the increased conjugations within the dipyrrinato anion certainly bring down the energy levels of the π orbitals of the ligands. The widened energy level difference between the d and π orbitals is bound to suppress the mixing of the orbitals from metal and ligand. This result, in addition to the decreased energy levels of π* orbitals of the ligands confirmed from the low reduction potentials, is beneficial to the ILCT rather than MLCT transition. Similar cases were also found in other Cu(I) complexes, in which the ILCT emission was observed in addition to the MLCT transition.[6,7]

Conclusion

A series of neutral mononuclear heteroleptic cuprous complexes based on the dipyrrinato anion have been synthesized and characterized. Crystallographic analyses reveal the cuprous complexes maintain a pseudo-tetrahedral coordination geometry except the complex **7a** with pyramidal structure due to steric hindrance. The studies of photophysical properties demonstrate that the low energy absorption and the emission of these complexes are assigned to ILCT of the dipyrrinato anion. The increased conjugation in the dipyrrin ligand after deprotonation decreases the energy level of π orbitals, which inhibits the effective spin–orbital coupling, leading to fluorescence rather than the expected phosphorescence. The experimental data and quantum chemical calculation supported the conclusions, which have also been

verified by other metal complexes. These results imply that the careful selection and rational design of ligands maintaining a matched energy level with metal d orbitals are the key factors to take full advantage of the triplet excited states in organic–metal complexes. Theoretical calculations in advance utilizing d orbital energy levels as a reference parameter should be a feasible route to prepare complexes with such desired properties.

Acknowledgements

This work was supported by the National Natural Science Foundation of China (Nos. 20874098 and 51073152) and the 973 Project (2009CB623600).

References

1 (*a*) D. R. McMillin and K. M. McNett, *Chem. Rev.*, 1998, **98**, 1201–1219; (*b*) A. Lavie-Cambot, M. Cantuel, Y. Leydet, G. Jonusauskas, D. M. Bassani and N. D. McClenaghan, *Coord. Chem. Rev.*, 2008, **252**, 2572–2584.
2 (*a*) D. V. Scaltrito, D. W. Thompson, J. A. O'Callaghan and G. J. Meyer, *Coord. Chem. Rev.*, 2000, **208**, 243–266; (*b*) N. Armaroli, *Chem. Soc. Rev.*, 2001, **30**, 113–124.
3 (*a*) D. G. Cuttell, S. M. Kuang, P. E. Fanwick, D. R. McMillin and R. A. Walton, *J. Am. Chem. Soc.*, 2002, **124**, 6–7; (*b*) Q. S. Zhang, Q. G. Zhou, Y. X. Cheng, L. X. Wang, D. G. Ma, X. B. Jing and F. S. Wang, *Adv. Mater.*, 2004, **16**, 432–436; (*c*) W. L. Jia, T. McCormick, Y. Tao, J. P. Lu and S. N. Wang, *Inorg. Chem.*, 2005, **44**, 5706–5712; (*d*) Q. S. Zhang, Q. G. Zhou, Y. X. Cheng, L. X. Wang, D. G. Ma, X. B. Jing and F. S. Wang, *Adv. Funct. Mater.*, 2006, **16**, 1203–1208; (*e*) N. Armaroli, G. Accorsi, M. Holler, O. Moudam, J. F. Nierengarten, Z. Y. Zhou, R. T. Wegh and R. Welter, *Adv. Mater.*, 2006, **18**, 1313–1316; (*f*) Z. S. Su, G. B. Che, W. L. Li, W. M. Su, M. T. Li, B. Chu, B. Li, Z. Q. Zhang and Z. Z. Hu, *Appl. Phys. Lett.*, 2006, **88**, 213508; (*g*) Q. S. Zhang, J. Q. Ding, Y. X. Cheng, L. X. Wang, Z. Y. Xie, X. B. Jing and F. S. Wang, *Adv. Funct. Mater.*, 2007, **17**, 2983–2990; (*h*) N. Robertson, *ChemSusChem*, 2008, **1**, 977–979; (*i*) Q. S. Zhang, Q. G. Zhou, Y. X. Cheng, D. G. Ma and L. X. Wang, *Chin. J. Appl. Chem.*, 2006, **23**, 570–572.
4 (*a*) A. Barbieri, G. Accorsi and N. Armaroli, *Chem. Commun.*, 2008, 2185–2193; (*b*) J. D. Slinker, J. Rivnay, J. S. Moskowitz, J. B. Parker, S. Bernhard, H. D. Abruña and G. G. Malliaras, *J. Mater. Chem.*, 2007, **17**, 2976–2988.
5 (*a*) H. V. Rasika Dias, H. V. K. Diyabalanage, M. A. Rawashdeh-Omary, M. A. Franzman and M. A. Omary, *J. Am. Chem. Soc.*, 2003, **125**, 12072–12073; (*b*) H. V. Rasika Dias, H. V. K. Diyabalanage, M. G. Eldabaja, O. Elbjeirami, M. A. Rawashdeh-Omary and M. A. Omary, *J. Am. Chem. Soc.*, 2005, **127**, 7489–7501; (*c*) S. B. Harkins and J. C. Peters, *J. Am. Chem. Soc.*, 2005, **127**, 2030–2031; (*d*) J. C. Deaton, S. C. Switalski, D. Y. Kondakov, R. H. Young, T. D. Pawlik, D. J. Giesen, S. B. Harkins, A. J. M. Miller, S. F. Mickenberg and J. C. Peters, *J. Am. Chem. Soc.*, 2010, **132**, 9499–9508; (*e*) A. J. M. Miller, J. L. Dempsey and J. C. Peters, *Inorg. Chem.*, 2007, **46**, 7244–7246; (*f*) J. H. Min, Q. S. Zhang, W. Sun, Y. X. Cheng and L. X. Wang, *Dalton Trans.*, 2011, **40**, 686–693.
6 (*a*) M. G. Crestani, G. F. Manbeck, W. W. Brennessel, T. M. McCormick and R. Eisenberg, *Inorg. Chem.*, 2011, **50**, 7172–7188; (*b*) G. F. Manbeck, W. W. Brennessel and R. Eisenberg, *Inorg. Chem.*, 2011, **50**, 3431–3441.
7 X. H. Liu, W. Sun, L. Y. Zou, Z. Y. Xie, X. Li, C. Z. Lu, L. X. Wang and Y. X. Cheng, *Dalton Trans.*, 2012, **41**, 1312–1319.
8 (*a*) A. Loudet and K. Burgess, *Chem. Rev.*, 2007, **107**, 4891–4932; (*b*) T. E. Wood and A. Thompson, *Chem. Rev.*, 2007, **107**, 1831–1861; (*c*) J. P. Strachan, D. F. O'Shea, T. Balasubramanian and J. S. Lindsey, *J. Org. Chem.*, 2000, **65**, 3160–3172; (*d*) N. Boens, V. Leen and W. Dehaen, *Chem. Soc. Rev.*, 2012, **41**, 1130–1172; (*e*) D. W. Cho, M. Fujitsuka, J. H. Ryu, M. H. Lee, H. K. Kim, T. Majima and C. Im, *Chem. Commun.*, 2012, **48**, 3424–3426.
9 I. V. Sazanovich, C. Kirmaier, E. Hindin, L. Yu, D. F. Bocian, J. S. Lindsey and D. Holten, *J. Am. Chem. Soc.*, 2004, **126**, 2664–2665.
10 C. Ikeda, S. Ueda and T. Nabeshima, *Chem. Commun.*, 2009, 2544–2546.
11 V. S. Thoi, J. R. Stork, D. Magde and S. M. Cohen, *Inorg. Chem.*, 2006, **45**, 10688–10697.
12 (*a*) J. D. Hall, T. M. McLean, S. J. Smalley, M. R. Waterland and S. G. Telfer, *Dalton Trans.*, 2010, **39**, 437–445; (*b*) T. M. McLean, D. M. Cleland, S. J. Lind, K. C. Gordon, S. G. Telfer and M. R. Waterland, *Chem.–Asian J.*, 2010, **5**, 2036–2046.
13 K. Hanson, A. Tamayo, V. V. Diev, M. T. Whited, P. I. Djurovich and M. E. Thompson, *Inorg. Chem.*, 2010, **49**, 6077–6084.
14 C. Bronner, S. A. Baudron, M. W. Hosseini, C. A. Strassert, A. Guenet and L. De Cola, *Dalton Trans.*, 2010, **39**, 180–184.
15 M. J. T. Frisch, G. W. Trucks, H. B. Schlegel, G. E. Scuseria, M. A. Robb, J. R. Cheeseman, J. A. Montgomery, Jr., T. Vreven, K. N. Kudin, J. C. Burant, J. M. Millam, S. S. Iyengar, J. Tomasi, V. Barone, B. Mennucci, M. Cossi, G. Scalmani, N. Rega, G. A. Petersson, H. Nakatsuji, M. Hada, M. Ehara, K. Toyota, R. Fukuda, J. Hasegawa, M. Ishida, T. Nakajima, Y. Honda, O. Kitao, H. Nakai, M. Klene, X. Li, J. E. Knox, H. P. Hratchian, J. B. Cross, V. Bakken, C. Adamo, J. Jaramillo, R. Gomperts, R. E. Stratmann, O. Yazyev, A. J. Austin, R. Cammi, C. Pomelli, J. W. Ochterski, P. Y. Ayala, K. Morokuma, G. A. Voth, P. Salvador, J. J. Dannenberg, V. G. Zakrzewski, S. Dapprich, A. D. Daniels, M. C. Strain, O. Farkas, D. K. Malick, A. D. Rabuck, K. Raghavachari, J. B. Foresman, J. V. Ortiz, Q. Cui, A. G. Baboul, S. Clifford, J. Cioslowski, B. B. Stefanov, G. Liu, A. Liashenko, P. Piskorz, I. Komaromi, R. L. Martin, D. J. Fox, T. Keith, M. A. Al-Laham, C. Y. Peng, A. Nanayakkara, M. Challacombe, P. M. W. Gill, B. Johnson, W. Chen, M. W. Wong, C. Gonzalez and J. A. Pople, *GAUSSIAN 03 (Revision A.9)*, Gaussian, Inc., Pittsburgh, PA, 2004.
16 *SADABS, Software for Empirical Absorption Correction, version 2.03*, Bruker AXS, Inc., Madison, WI, 2002.
17 G. M. Sheldrick, *Acta Crystallogr., Sect. A: Found. Crystallogr.*, 2007, **64**, 112–122.
18 A. D. Abell, B. K. Nabbs and A. R. Battersby, *J. Am. Chem. Soc.*, 1998, **120**, 1741–1746.
19 R. W. Boyle, C. Bruckner, J. Posakony, B. R. James and D. Dolphin, *Org. Synth.*, 1999, **76**, 287–293.
20 A. Burghart, H. J. Kim, M. B. Welch, L. H. Thoresen, J. Reibenspies, K. Burgess, F. Bergstrom and L. B. A. Johansson, *J. Org. Chem.*, 1999, **64**, 7813–7819.
21 L. J. Jiao, W. D. Pang, J. Y. Zhou, Y. Wei, X. L. Mu, G. F. Bai and E. H. Hao, *J. Org. Chem.*, 2011, **76**, 9988–9996.
22 N. Armaroli, G. Accorsi, G. Bergamini, P. Ceroni, M. Holler, O. Moudam, C. Duhayon, B. Delavaux-Nicot and J. F. Nierengarten, *Inorg. Chim. Acta*, 2007, **360**, 1032–1042.
23 (*a*) L. Jiao, C. Yu, J. Li, Z. Wang, M. Wu and E. Hao, *J. Org. Chem.*, 2009, **74**, 7525–7528; (*b*) H. L. Kee, C. Kirmaier, L. H. Yu, P. Thamyongkit, W. J. Youngblood, M. E. Calder, L. Ramos, B. C. Noll, D. F. Bocian, W. R. Scheidt, R. R. Birge, J. S. Lindsey and D. Holten, *J. Phys. Chem. B*, 2005, **109**, 20433–20443.
24 (*a*) E. Lager, J. Z. liu, A. Aguilar-Aguilar, B. Z. Tong and E. Peña-Cabrera, *J. Org. Chem.*, 2009, **74**, 2053–2058; (*b*) S. Goeb and R. Ziessel, *Org. Lett.*, 2007, **9**, 737–740; (*c*) T. S. Teets, D. V. Partyka, A. J. Esswein, J. B. Updegraff, M. Zeller, A. D. Hunter and T. G. Gray, *Inorg. Chem.*, 2007, **46**, 6218–6220.
25 (*a*) J. Karolin, L. B. A. Johansson, L. Strandberg and T. Ny, *J. Am. Chem. Soc.*, 1994, **116**, 7801–7806; (*b*) W. W. Qin, M. Baruah, M. Van der Auweraer, F. C. De Schryver and N. Boens, *J. Phys. Chem. A*, 2005, **109**, 7371–7384; (*c*) K. Kim, C. Jo, S. Easwaramoorthi, J. Sung, D. H. Kim and D. G. Churchill, *Inorg. Chem.*, 2010, **49**, 4881–4894.
26 S. M. Kuang, D. G. Cuttell, D. R. McMillin, P. E. Fanwick and R. A. Walton, *Inorg. Chem.*, 2002, **41**, 3313–3322.
27 (*a*) J. Brooks, Y. Babayan, S. Lamansky, P. I. Djurovich, I. Tsyba, R. Bau and M. E. Thompson, *Inorg. Chem.*, 2002, **41**, 3055–3066; (*b*) M. V. Kulikova, K.P. Balashev, P.I. Kvam and J. Songstad, *Russ. J. Gen. Chem.*, 2000, **70**, 163–170.
28 F. Li, S. I. Yang, Y. Ciringh, J. Seth, C. H. Martin, D. L. Singh, D. Kim, R. R. Birge, D. F. Bocian, D. Holten and J. S. Lindsey, *J. Am. Chem. Soc.*, 1998, **120**, 10001–10017.
29 L. Qin, Q. S. Zhang, W. Sun, J. Y. Wang, C. Z. Lu, Y. X. Cheng and L. X. Wang, *Dalton Trans.*, 2009, 9388–9391.